

Tracking of Volcanic Ash Emanated through Shinmoedake Eruption by Using MTSAT Split-window Imagery

Toshihisa Itano, Yuki Matsuura and Takao Eguchi

Dept. Earth & Ocean Sciences, National Defense Academy, Yokosuka, Japan

(E-Mail: itano@nda.ac.jp)

Abstract

Slight difference in emissivity between IR1 (10.3-11.3 μ m) and IR2 (11.5-12.5 μ m) channel against mineral particles enables us to discriminate volcanic ash clouds from water clouds by calculating difference on brightness temperature between these two split-window channels (Patra 1989ab). By using this technique, the evolution of the volcanic ash emanated through Shinmoedake eruption on January 26, 2011 is tracked over the MTSAT imagery. This event was the first severe volcanic activity since the MTSAT was launched in 2005, and the high-accuracy (10-Bit) split-window radiometer equipped on it successfully detects the volcanic ash clouds as regions of negative brightness temperature difference, i.e. $T_b(ir1)-T_b(ir2)<0$. A consecutive look of the split-window difference imagery reveals eastward diffusion of volcanic ash. But due to the wind shear in the westerlies with height and the difference in the height of plumes emanate from each eruption events, the spreading area of the volcanic ash bifurcates into two directions, forming a pitchfork shape elongating from the volcano. Some other statistical results are also calculated from the MTSAT HRIT dataset.

1. Introduction

Explosive volcanic eruption of Shinmoedake [1,421 m] (Fig.1), one of the peaks of the Mt. Kirishima cluster of volcanoes located on the southern part of Kyushu Island in Japan, had occurred in January 26, 2011. It was the first explosive eruption of this volcano since 1959, and undoubtedly the largest one occurred in Japan for the last decade. The eruption not only caused serious damages on the area surrounding the volcano through a large amount of volcanic fallout and air vibrations, but also affected the area far from the volcano through the long-term transport of the volcanic ash emanated from the eruption. Fortunately, in this case, the newly equipped split-windows sensor on the MTSAT enables us to track the diffusion of the ash on the planar images obtained by the sensor after simple mathematical operations. In this study, we carry out a case study of tracking the volcanic ash emanated from this eruption on the MTSAT split-window imagery.



Fig.1 Geography

2. History of the MTSAT / GMS

Before the analysis, we would like to introduce the background of the present study in connection with the history of the MTSAT / GMS. Refer to Fig.2 for the explanation below. Until GMS-4, the satellites had only two sensors equipped on them: i.e. one sensor in the visible channel (VIS), and the other in the infrared channel (IR). On the next generation satellite of GMS-5, the water vapor channel (WV) is newly prepared and the infrared channel was divided into two parts, i.e. IR1 (10.3-11.3 μm) and IR2 (11.5-12.5 μm), forming the split-window channel. Unfortunately, all data disseminated from the GMS-5 was provided with 8-Bit (256 tones), which was insufficient for calculating the difference of two split-window images. In addition, the GMS series was a spin-stabilized satellite. Therefore, its navigation was not satisfactory especially for time-dependent image display. In this respect, the MTSAT, released in 2005, has tri-axial stabilization and the gradation of all channel increases to 10-Bit (1024 tones). At this point, it becomes possible to calculate the difference of two split-window

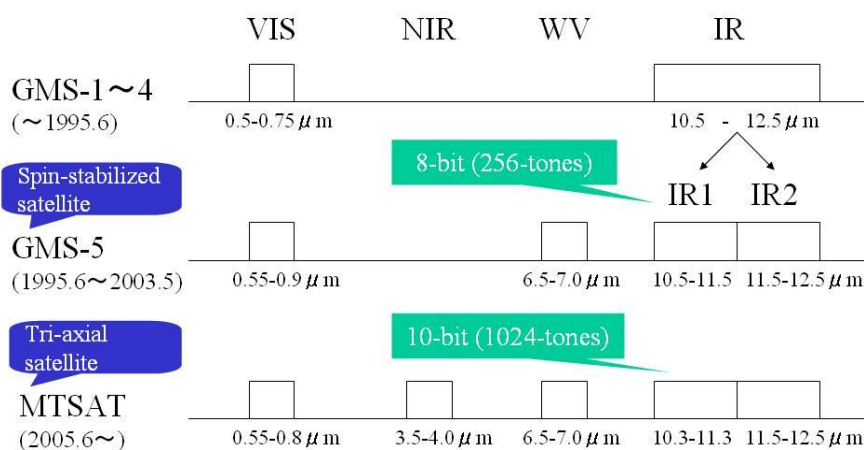


Fig.2 Spectral band width of the MTSAT & GMS.

images, which is necessary to discriminate the volcanic ash clouds from water clouds, with sufficient accuracy. Here, we would like to note that the volcanic eruption of Shinmoedake was the first tremendous volcanic event occurred in Japan since the MTSAT was launched.

3. Data

National Defense Academy (NDA) has operated the MDUS (Medium-scale Data Utilization Stations) for the MTSAT since 2006. Data used in this study is the HRIT (High Rate Image Transmission) of the MTSAT-1R received and collected at NDA. In the 5 channels prepared in the MTSAT-1R, we pick up two channels constituting the split-window channel, i.e. IR1 (10.3-11.3 μ m) and IR2 (11.5-12.5 μ m). Their spatial resolution is 4 km at the sub-point of the satellite (140° E). As for their time resolution, the MTSAT performs the half-disk observation of the earth, in addition to the hourly full-disk observation, at the interval of 1 hour. So, the frequency of the observation over the northern hemisphere is twice an hour. In this study, however, we adopt the full earth's disk images alone. Thus the time intervals of the successive satellite images are 1 hour. The gradation of each image is, as mentioned above, 10-bit (1024 tones). Period of the analysis is set to start January 25, 2011, i.e. one day before the eruption.

The aerological data at Kagoshima, locating about 50 km southwest of Shinmoedake (Fig.1), is also used to make up for the analysis. The elements of measurement are temperature, dew point temperature, pressure, wind speed & direction. The time interval is twice a day [09 & 21 JST (UTC+9)].

4. Principle

Since the wavelength bands of IR1 (10.3-11.3 μ m) and IR2 (11.5-12.5 μ m) channels are adjacent with each other, most substances measured by these two channels are viewed in the same way (see Fig.3). However, due to slight differences in the radiation characteristics between these two split-window channels against mineral particles, volcanic ash clouds can be clearly distinguished from water clouds on the difference image of IR1 and IR2 (Patra 1989ab). This may be understandable in the following way. For the area covered by cirrus or the humid clear-sky region, the radiation observed at IR1 channel is slightly larger than that at IR2 channel. On the contrary, for the area covered by volcanic ash clouds or mineral dust, the radiation observed at IR2 channel is slightly larger than that at IR2 channel. Thus, these clouds and substances are discriminated by considering the sign of the brightness temperature difference (BTD) of IR1 and IR2, i.e.

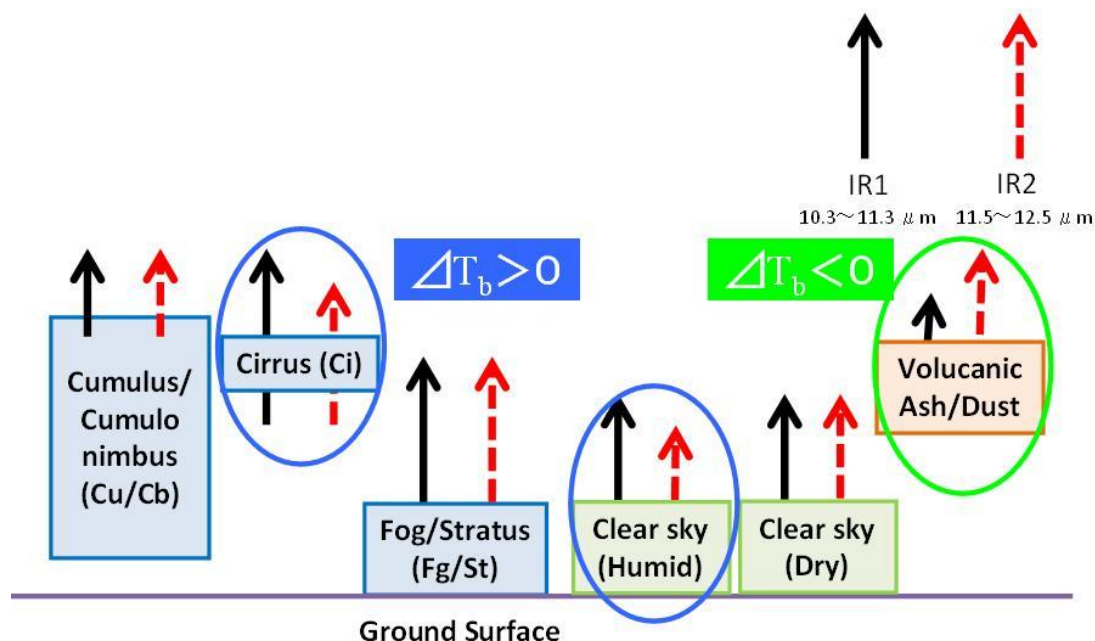


Fig.3 Radiation characteristics for various substances.

$$\Delta T_b = T_b (IR1) - T_b (IR2)$$

where $\Delta T_b > 0$ [K] indicates the area of high humidity or cirrus clouds whereas $\Delta T_b < 0$ [K] indicates the area covered by volcanic ash or mineral dust.

For the actual application of detecting volcanic ash, threshold of 0 [K] is not necessarily enough to discriminate volcanic ash alone. So, we supplementary adopt more severe threshold of $\Delta T_b < -0.5, -1.0, -2.0, -4.0$ and -6.0 [K].

As for coloring of the BTD images, we assign black to positive BTD and white to negative BTD. Thus, volcanic ash clouds are colored with white on the BTD images.

5. Results

5.1 Example of the BTD image

One example of discriminating volcanic ash from other types of clouds is introduced. Figure 4 shows IR1, IR2, and BTD images just after the first explosive eruption (17:30 JST, January 26, 2011). The IR1 and IR2 images are visible in the same way, where clouds associated with Shinmoedake eruption is seen in the same way as other various types of clouds. There, it is difficult to discriminate volcanic ash clouds alone. However, as seen in Fig.4c, such clouds are readily discriminated on the BTD images.

5.2 Statistics

Next, statistics of volcanic ash clouds on the BTD imagery are obtained. These

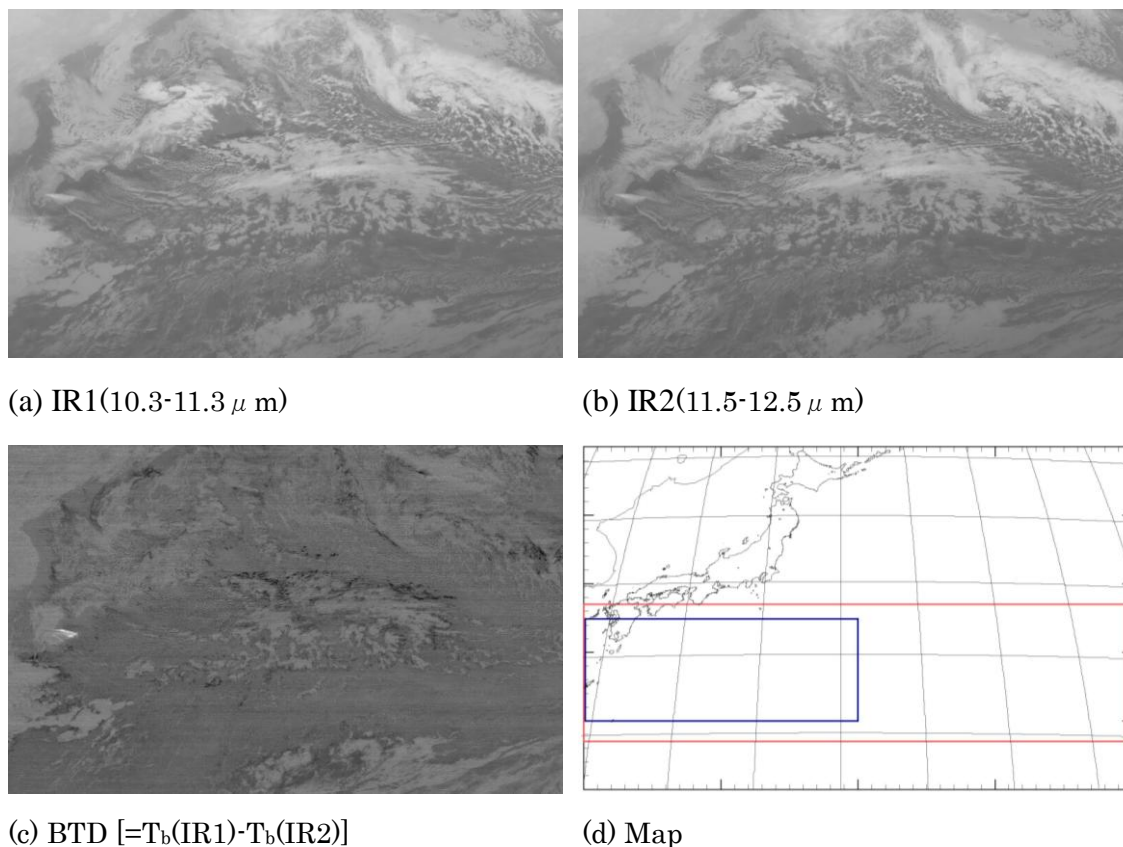


Fig.4 IR1, IR2 & BTM images of the MTSAT at 17:30 JST(UTC+9), January 26, 2011.

statistics are calculated within the smallest rectangle shown in Fig.4d. First of all, the accumulated time covered by volcanic ash clouds during 52 hours since January 26, 06 JST is provided. This is done by counting a number of times satisfying negative BTM at each pixel at the time interval of one hour. The result is shown in Fig.5a, where we will see a pitchfork-shaped trace of volcanic ash elongating from Shinmoedake and roughly spreading into two directions. Unfortunately, signals irrelevant to volcanic ash are also detected in the figure. Such noisy signals, however, can be removed by increasing the threshold of detecting volcanic ash clouds at least to $\Delta T_b < -0.5$ [K] (Fig.5b). The aerological data at Kagoshima reveals that the upper air condition was quite steady during the period before and after the eruption: the axis of the jet stream exceeding 80 m/s existed at the height of 11 km, whose direction is westerly above 5 km height and northwesterly or northerly below it (Fig.6). Comparison with this aerological data suggests that the trace of volcanic ash extending southwestward was brought by the eruptions whose plume height was less than 5 km. Meanwhile, more strong eruptions whose plume penetrated much higher than 5 km height were supposed to cause the ESE-ward trace of volcanic ash. In this case, the volcanic ash was transported

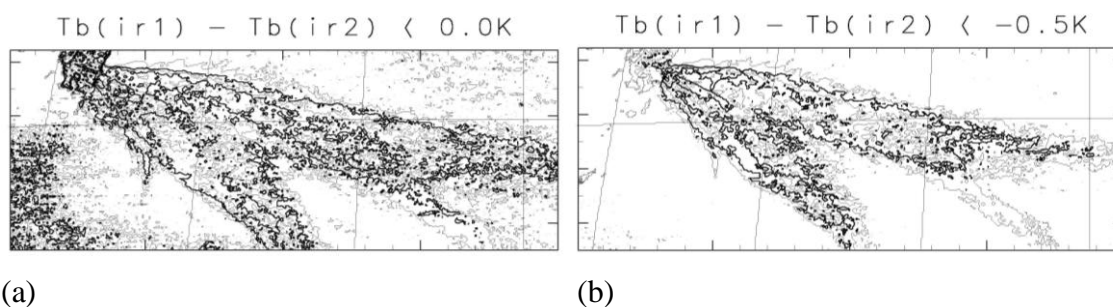


Fig.5 Accumulated time covered by volcanic ash during January 26 (15 JST)-28 (20 JST) [total 52 hours] calculated with (a) $\Delta T_b < 0$ [K] and (b) $\Delta T_b < -0.5$ [K].

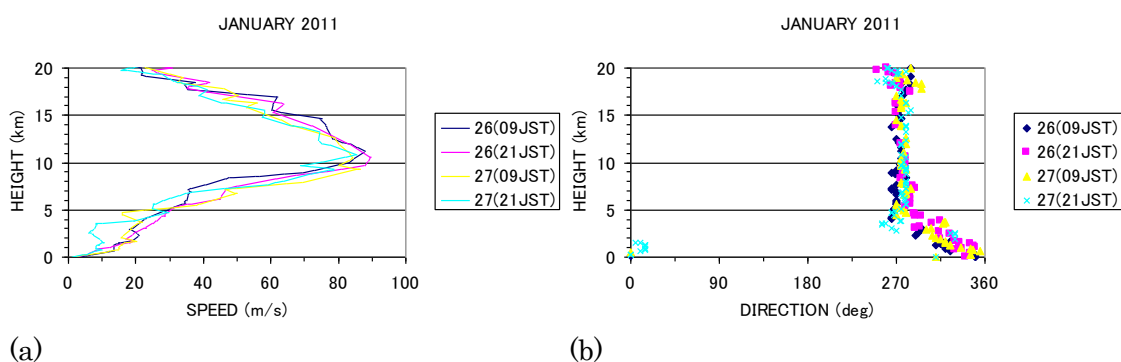


Fig.6 Aerological data at Kagoshima for (a) wind speed and (b) direction.

westward at the very first of such eruptions and then moved southward when it fell out into the lower atmosphere where the westerly jet had northerly component.

Next, the time variations of the volcanic ash clouds on the BTD imagery are obtained under various thresholds. Figure 7 shows the time series of the area covered by volcanic ash clouds and, as an indicator of the cloud height, its mean brightness temperature. According to Fig.7a, the maximum cloud cover occurred after 8 hours from the eruption and thereafter the area decreased quickly with time. This implies the volcanic ash went out from the range of interest until one day after the eruption. Meanwhile, the minimum brightness temperature was seen after several hours from the eruption and, after that, raised (i.e. decreased cloud height) with time (Fig.7b).

Finally, we pick up top ten pixels of small BTD values. Figure 8a is the time series of the BTD values of such ten pixels. The BTD of each pixel dropped quickly after the eruption and recorded its minima reaching -8 [K] at several hours later. The BTD kept low value intact until around the end of January 26. However, the volcanic ash emanated from the eruption might be the densest at the very first of the eruption. So, if the BTD is related to the quantity of the diffused volcanic ash, the BTD minima should

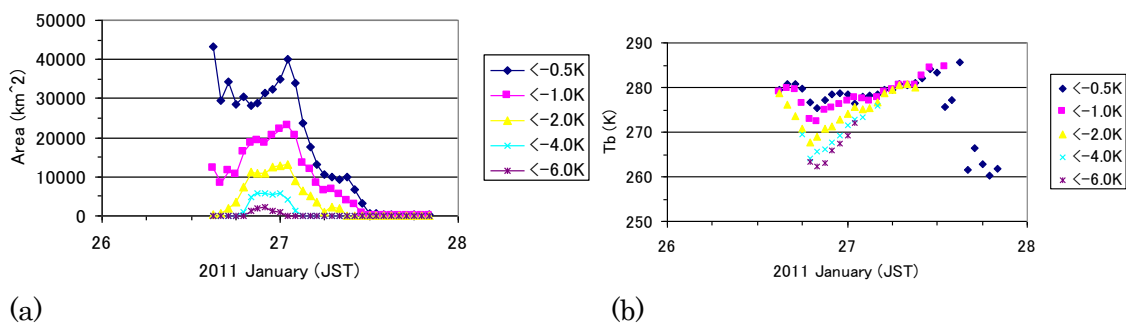


Fig.7 Time series of (a) the area of the volcanic ash and (b) its mean brightness temperature obtained with various thresholds.

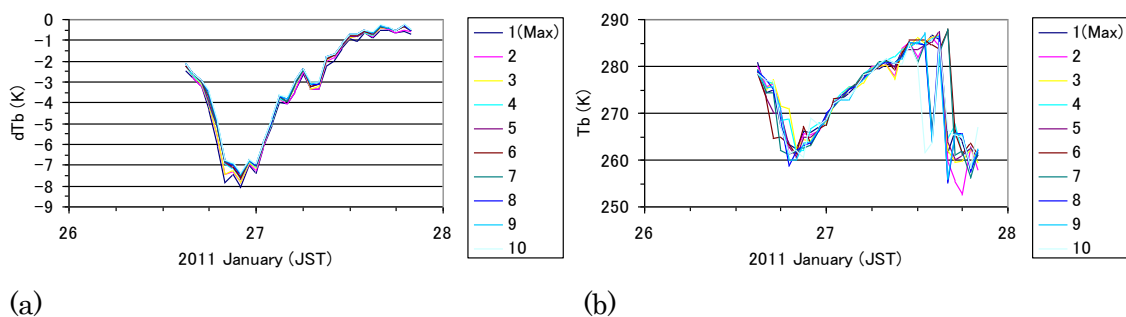


Fig.8 Time series of (a) the BTD and (b) the brightness temperature of the top ten pixels with the smallest BTD values

be analyzed at the time of the eruption. In this respect, there are some problems to detect nascent eruption clouds on the BTD imagery. Meanwhile, Fig.8b is the time series of corresponding brightness temperature. The brightness temperature minima were observed at seven hours after the eruption, and then the temperature increased gradually with time, i.e. the height z of the pixels decreased with time. Here, it is remarkable that the brightness temperature minima of 260 [K] correspond to $z \sim 3,700$ m and it is apparently much lower than the actual volcanic plume of Shinmoedake on January 26. This fact seems to indicate that the volcanic plumes are thermally in-equilibrium with the surrounding environment.

6. Summary

The evolution of the volcanic ash emanated from the explosive Shinmoedake eruption on January 2011 is tracked on the MTSAT infrared images. The high-accuracy (10-bit) split-window radiometer equipped on the MTSAT enable us to detect volcanic ash clouds successfully as regions of negative BTD (Brightness Temperature Difference), i.e. $T_b(\text{IR1}) - T_b(\text{IR2}) < 0$, as proposed by Prata (1989ab). A consecutive

look of the BTM imagery reveals eastward diffusion of volcanic ash, forming a pitchfork-shaped trace elongating from the volcano. Comparison between the aerological data at Kagoshima implies the wind shear in the westerly wind with height and the difference of individual plume height with eruptions, the spreading are of the volcanic ash bifurcates mainly into two directions. In contrast to the above successful results, several subjects to be solved are also found especially at the early stage of volcanic eruptions.

References

- Prata, A.J., 1989a: Observations of volcanic ash clouds in the 10-12 μ m window using AVHRR/2 data. *Int. J. Remote Sensing*, **10**, 751-761.
- Prata, A.J., 1989b: Infrared radiation transfer calculations for volcanic ash clouds. *Geophys. Res. Lett.*, **16**, 1,293-1,296.